Immunity
Article

Deletion of *Notch1* Converts Pro-T Cells to Dendritic Cells and Promotes Thymic B Cells by Cell-Extrinsic and Cell-Intrinsic Mechanisms

Thorsten B. Feyerabend,[1] Grzegorz Terszowski,[1] Annette Tietz,[1] Carmen Blum,[1] Hervé Luche,[1] Achim Gossler,[2] Nicholas W. Gale,[3] Freddy Radtke,[4] Hans Jörg Fehling,[1] and Hans-Reimer Rodewald[1,*]
[1]Institute for Immunology, University of Ulm, D-89081 Ulm, Germany
[2]Institute for Molecular Biology, Medizinische Hochschule Hannover, D-30625 Hannover, Germany
[3]Regeneron Pharmaceuticals, 777 Old Saw Mill River Road, Tarrytown, NY 10591, USA
[4]Ecole Polytechnique Fédérale de Lausanne, Swiss Institute for Experimental Cancer Research, Chemin de Boveresses 155, CH-1066 Epalinges, Switzerland
*Correspondence: hans-reimer.rodewald@uni-ulm.de
DOI 10.1016/j.immuni.2008.10.016

SUMMARY

Notch1 signaling is required for T cell development and has been implicated in fate decisions in the thymus. We showed that Notch1 deletion in progenitor T cells (pro-T cells) revealed their latent developmental potential toward becoming conventional and plasmacytoid dendritic cells. In addition, Notch1 deletion in pro-T cells resulted in large numbers of thymic B cells, previously explained by T-to-B cell fate conversion. Single-cell genotyping showed, however, that the majority of these thymic B cells arose from Notch1-sufficient cells by a cell-extrinsic pathway. Fate switching nevertheless exists for a subset of thymic B cells originating from Notch1-deleted pro-T cells. Chimeric mice lacking the Notch ligand delta-like 4 (Dll4) in thymus epithelium revealed an essential role for Dll4 in T cell development. Thus, Notch1-Dll4 signaling fortifies T cell commitment by suppressing non-T cell lineage potential in pro-T cells, and normal Notch1-driven T cell development repels excessive B cells in the thymus.

INTRODUCTION

The Notch signaling pathway guides cell-fate decisions in multiple developmental processes (Artavanis-Tsakonas et al., 1999; Dumortier et al., 2005). In hematopoiesis, Notch1 signaling can influence the "balance" between T cell and B cell development (Jenkinson et al., 2006; Maillard et al., 2005; Osborne, 2000; Radtke et al., 2004; Robey and Bluestone, 2004; Rothenberg et al., 2008; Tanigaki and Honjo, 2007). Overexpression or constitutive activation of Notch1 signaling promotes T cell development, blocks B cell development (Pui et al., 1999), and is frequently associated with T cell leukemia (Aster et al., 2008). In contrast, deletion of *Notch1* or inhibition of Notch1 signaling in hematopoietic stem cells (HSCs) blocks T cell development in favor of unusually high numbers of thymic B cells (Izon et al., 2002; Koch et al., 2001; Maillard et al., 2004; Radtke et al., 1999; Wilson et al., 2001).

The abundance of B cells in the thymus under conditions of impaired Notch1 signaling has been interpreted as evidence for cell-intrinsic fate switching of lymphoid or perhaps T cell-committed progenitors toward becoming B cells. Such cell-autonomous T-to-B cell conversion implies that Notch1-expressing progenitors, destined to become T cells under Notch1 signaling, transdifferentiate to become B cells in the absence of Notch1 signaling. A less considered possibility is that B cells appearing in the thymus under conditions of loss of Notch1 function may not share a precursor-product relationship with *Notch1*-deleted progenitors. Such B cells would be developmentally unrelated to the T cell pathway, and they might fill available space in the thymus. Direct experimental evidence distinguishing between these possibilities is lacking (Maillard et al., 2005). A question closely related to the plasticity of thymic precursors is their potential for becoming dendritic cells (DCs) (Shortman and Naik, 2007). It is interesting to consider an involvement of Notch1 in progenitor T cell (pro-T cell)-to-DC fate decisions in the thymus. Inactivation of Notch1 signaling after the T-B cell bifurcation and prior to $CD4^{-}CD8^{-}$ double-negative (DN) $CD25^{+}$ stages in the thymus, when B cells can no longer arise experimentally (Sambandam et al., 2005; Schmitt et al., 2004), might provide a clue for these questions. However, relevant pathways from the HSC up to the pro-T stage are largely uncharted and hence difficult to manipulate in vivo (Benz et al., 2008; Bhandoola et al., 2007; Petrie and Kincade, 2005; Rodewald, 1995).

We have generated a Cre-recombinase (Cre)-deleter mouse that shows "T cell-biased" Cre activity. This strain permits preferential deletion of floxed (fl) genes in the T cell pathway downstream of the physiological T-B cell bifurcation. Using the *ROSA26-RFP* (*RFP*) reporter mouse expressing the tandem-dimer red fluorescent protein (RFP) gene in a Cre-dependent manner (Luche et al., 2007), we demonstrated RFP expression in ~45% of DN1 Kit^{+} T cell progenitors, and it was maximal (~90%) as of the DN2 stage. Disruption of *Notch1* in pro-T cells with this Cre line impaired T cell development and was associated with increased numbers of thymic B cells, as expected. In conflict with the idea of fate conversion as the major, if not only, mechanism underlying the generation of additional thymic B cells under conditions of *Notch1* deficiency, we found that a large fraction of thymic B cells arose from non-*Notch1*-deleted

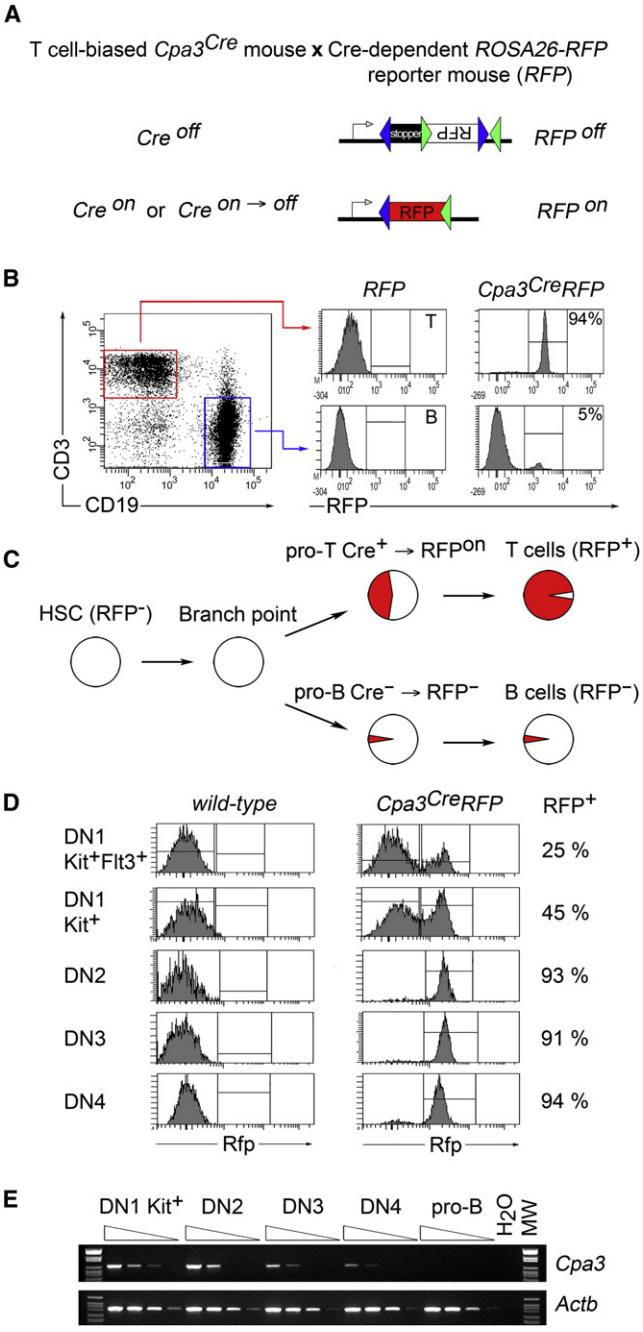

Figure 1. Experimental Setup and T Cell-Biased Cre-Labeling Pattern in *Cpa3*^{Cre} Mice

(A) *Cpa3*^{Cre} mice were crossed with Cre-dependent *ROSA26-RFP (RFP)* reporter mice. The *RFP* reporter locus harbors two pairs of loxP sites (represented by green and blue triangles) that are pairwise compatible. Permanent RFP expression is achieved via Cre-dependent recombination steps involving inversion of the *RFP* gene and deletion of the stopper (Luche et al., 2007).

(B) Spleen cells from *Cpa3*^{Cre}*RFP* and *RFP* control mice were stained for CD3 versus CD19 expression, and RFP expression was analyzed after gating on CD3$^+$ T cells and CD19$^+$ B cells. Data are representative of seven independent experiments.

(C) This T cell-biased Cre activity preferentially labels the T cell lineage downstream of the physiological T-B cell bifurcation ("branch point"). Frequencies of RFP-marked cells in T cell and B cell development are schematically depicted.

progenitors. Hence, these B cells are influenced cell-extrinsically by loss of *Notch1* in T cell progenitors. The second key finding uncovered by deletion of *Notch1* at the pro-T cell stage is a *Notch1*-dependent, cell-intrinsic redirection of cells out of the T cell pathway into thymic DCs of conventional and plasmacytoid lineages. These experiments expand the range of developmental processes that are regulated by Notch1 via cell-intrinsic and cell-extrinsic mechanisms in the thymus. Finally, we provide genetic evidence that the Notch ligand delta-like 4 (Dll4) is crucial for T cell development in vivo. Thus, we report a crucial function of Notch1 in limiting development of pro-T cells toward DC and B cell lineages in the thymus and reveal an unexpected capacity of thymic niches, deserted by Notch1-deficient thymocytes, to host B cells that do not arise in the T cell pathway.

RESULTS

Cpa3^{Cre} Labels the Vast Majority of T Cells Downstream of the T-B Cell Bifurcation

For quantifying hematopoietic pathways in vivo, mice expressing Cre in lineage-restricted loci are useful for Cre-driven fate mapping and for deletion of floxed genes (Rajewsky et al., 1996). We constructed by gene targeting a knockin mouse in which Cre expression is under the control of the *Cpa3* gene encoding mast cell carboxypeptidase A (Mc-cpa). *Cpa3* is considered a mast cell-specific gene (Reynolds et al., 1989) and is expressed in this lineage from the progenitor stage onward (Rodewald et al., 1996). To assess the labeling pattern of Cre, we crossed *Cpa3*^{Cre} mice with Cre-dependent *RFP* reporter mice. In *Cpa3*^{Cre}*RFP* mice, all cells expressing Cre at one point in ontogeny, as well as their progeny, were permanently labeled by RFP (Figure 1A). A survey of hematopoietic lineages showed, interestingly, frequencies of RFP$^+$ CD3$^+$ T cells in the spleen in the order of 90% (88% [mean] ± 5% [one standard deviation]; n = 7 mice). Frequencies of RFP$^+$ CD19$^+$ splenic B cells were, by comparison, very low (4.6% ± 2.0%; n = 7) (Figure 1B). Differential marking of T cells and B cells was recapitulated by transplantation of lymphocyte-depleted bone marrow cells from *Cpa3*^{Cre}*RFP* into alymphoid *Rag2*$^{-/-}$*Il2rg*$^-$ hosts (data not shown), demonstrating that the T-over-B cell bias was ongoing in adult T cell and B cell development.

Preferential T cell labeling implied that Cre was predominantly active downstream of the physiological split between T and B cell lineages (Figure 1C). Next, we searched for the stage in T cell development in which labeling first became apparent. In CD4$^+$CD8$^+$ double-positive (DP) and CD4$^+$CD8$^-$ and CD4$^-$CD8$^+$ single-positive (SP) thymocyte subsets, frequencies of RFP$^+$ cells were as high as in peripheral T cells (data not shown). Similarly, ~90% of DN2 (90.2% ± 2.7%; n = 4), DN3 (93.9% ± 1.5%;

(D) Subsets of DN cells, defined as Lin$^-$ DN1 Kit$^+$Flt3$^+$, Lin$^-$ DN1 Kit$^+$, DN2, DN3, and DN4, from *Cpa3*^{Cre}*RFP* and wild-type control mice were analyzed for RFP expression. Mice were between 5 weeks and 3 months old, and the RFP labeling pattern was age independent (data not shown). Data are representative of at least three independent experiments.

(E) DN subsets were purified from normal mice by cell sorting and analyzed by RT-PCR for endogenous expression of *Cpa3* (top) and *Actb* (bottom). The triangle represents 10-fold dilutions of the cDNAs. Data from one of two independent experiments are shown.

n = 4), and DN4 (89.0% ± 2.5%; n = 4) stages were RFP$^+$ (Figure 1D). Interestingly, labeling was evident already in ~25% (22.4% ± 4.1%; n = 3) of the earliest pro-T cells, defined as lineage-marker-negative (Lin$^-$) DN1 Kit$^+$ Flt3$^+$ (Sambandam et al., 2005), and in ~45% (46.2% ± 7.6%; n = 4) of the total Lin$^-$ DN1 Kit$^+$ pro-T cell population (Figure 1D). Labeling was saturated as of DN2 and remained high in subsequent stages.

Because *Cpa3* has been considered a mast cell-specific gene, the very early and near-complete labeling of thymocytes was unexpected and raised the question of whether expression of *Cpa3^{Cre}* paralleled expression of the endogenous *Cpa3* locus in the thymus. To this end, DN stages sorted from normal mice were analyzed by reverse transcriptase-polymerase chain reaction (RT-PCR). To exclude potential thymus-resident mast cells, we included FcεRI antibody in the Lin cocktail. The endogenous *Cpa3* gene was transcribed in DN1 Kit$^+$, in DN2, and, to a lesser extent, in DN3 and DN4, but not in CD19$^+$Kit$^+$ pro-B cells (Figure 1E). Mast cell genes, including *Cpa3*, are expressed in early T cell progenitors (Taghon et al., 2007). According to our data, at least 90% of all thymocytes pass through a *Cpa3*-expressing stage. Frequencies of RFP$^+$ cells among bone marrow stem cells and progenitor populations are shown in Figure S1A (available online), and they are further considered in the Supplemental Results. Thus, *Cpa3^{Cre}* mice label the earliest stages of T cell development in the thymus and, possibly, in thymus-colonizing progenitors, and they may hence be useful for genetically manipulating pro-T cells in vivo.

Deletion of *Notch1* by *Cpa3^{Cre}* Impairs Pro-T Cell Development

Deletion of *Notch1* in HSCs by *Mx^{Cre}* blocked T cell development and raised thymic B cell numbers (Radtke et al., 1999). In this case, all progeny of *Notch1*-deleted HSCs, including B cells, are *Notch1* deleted. Ontogenetically later ablation of *Notch1* by *Lck^{Cre}* perturbed thymocyte development without increasing thymic B cells (Wolfer et al., 2002). Using *Cpa3^{Cre}*, we addressed consequences of *Notch1* deletion en route from HSCs to T cells and, importantly, downstream of the T-B cell split. To this end, we generated *Notch1$^{fl/+}$Cpa3^{Cre}* and *Notch1$^{fl/fl}$Cpa3^{Cre}* mice. Deletion of the floxed first exon of the *Notch1* gene rendered the mutant allele nonfunctional (Figure 2A) (Radtke et al., 1999). If T cell development were impaired and thymic B cells increased in *Notch1$^{fl/fl}$Cpa3^{Cre}* mice, the *Notch1* genotype of thymic B cells should be informative about the mechanism of their generation.

Because Cre fate-mapped approximately 90%, but not all, thymocytes (Figure 1), early T cell development was severely diminished, but not fully arrested, in *Notch1$^{fl/fl}$Cpa3^{Cre}* mice. Total thymocyte cellularity was reduced by 65% in *Notch1$^{fl/fl}$Cpa3^{Cre}* mice (0.38 × 10^8 thymocytes) as compared to that in *Notch1$^{fl/+}$Cpa3^{Cre}* mice (1.1 × 10^8 thymocytes) (Figure 2B). Percentages of DP thymocytes were altered from 80% ± 4.6% (n = 4) in *Notch1$^{fl/+}$Cpa3^{Cre}* mice to 65% ± 6.0% (n = 6) in *Notch1$^{fl/fl}$Cpa3^{Cre}* mice, and SP stages were correspondingly increased in *Notch1$^{fl/fl}$Cpa3^{Cre}* mice. The Notch1 dependency of pro-T cell development (Sambandam et al., 2005; Tan et al., 2005) was confirmed by the reduced percentages of DN1a and DN1b cells (Porritt et al., 2004; also referred to as early thymic progenitors [ETPs] in Bhandoola et al., 2003) in *Notch1$^{fl/fl}$Cpa3^{Cre}* mice (Figures 2C and 2D). Percentages of DN CD25$^+$ cells were reduced by more than 50% in *Notch1$^{fl/fl}$Cpa3^{Cre}* mice (Figure 2E). Absolute numbers of DN1 Kit$^+$, DN2 Kit$^+$, and DN CD25$^+$ cells were progressively diminished along early thymocyte maturation (Figure 2F). Collectively, obstructed DN development in *Notch1$^{fl/fl}$Cpa3^{Cre}* mice was consistent with continuously required Notch1 signaling during T cell development (Ciofani and Zuniga-Pflucker, 2007).

Deletion of *Notch1* by *Cpa3^{Cre}* Promotes Two B Cell Populations in the Thymus

Because deletion of *Notch1* at the HSC stage (Radtke et al., 1999), but not at the DN2 and DN3 stages (Wolfer et al., 2002), led to increased thymic B cell numbers, we next analyzed whether deletion of *Notch1* by *Cpa3^{Cre}* resulted in the appearance of more thymic B cells. Thymi from *Notch1$^{fl/+}$Cpa3^{Cre}* and *Notch1$^{fl/fl}$Cpa3^{Cre}* mice were analyzed for percentages of CD19- and B220-expressing B cells among DN cells. In the *Notch1$^{fl/+}$Cpa3^{Cre}* control thymus, B cells were rare (Figure 3A, left panel, and Figures 3D and 3E), and essentially all of these were CD19^{hi}B220^{hi} cells (termed CD19^{hi}). In contrast, in *Notch1$^{fl/fl}$Cpa3^{Cre}* mice, percentages of thymic B cells were increased approximately 10-fold (Figure 3A, right panel). These B cells consisted of a major CD19^{hi} population and an additional CD19^{lo}B220^{lo} (termed CD19^{lo}) population. CD19^{lo} and CD19^{hi} B cells were also found in the bone marrow (Figure 3B), where the CD19 and B220 staining pattern was indistinguishable between *Notch1$^{fl/+}$Cpa3^{Cre}* and *Notch1$^{fl/fl}$Cpa3^{Cre}* mice (data not shown). CD19^{hi} B cells from thymus and bone marrow of *Notch1$^{fl/+}$Cpa3^{Cre}* and *Notch1$^{fl/fl}$Cpa3^{Cre}* mice had a mature B2 B cell phenotype (Figure 3C). CD19^{lo} thymic B cells, most of which were IgM$^-$ (Figure 3C), included pro-B cell (Kit$^+$CD25$^-$) and precursor B cell (pre-B cell; Kit$^-$CD25$^+$) phenotypes (Supplemental Results and Figure S2). Because percentages of thymic B cells can be elevated because of the paucity of thymocytes (Figure 2B), absolute numbers of total thymic B cells (Figure 3D) and of CD19^{lo} and CD19^{hi} subsets (Figure 3E) were compared in *Notch1$^{fl/+}$Cpa3^{Cre}* mice and *Notch1$^{fl/fl}$Cpa3^{Cre}* mice. Total numbers of B cells varied over a wide range but increased overall by 10-fold in *Notch1$^{fl/fl}$Cpa3^{Cre}* mice. Further dissection revealed a larger absolute increment for CD19^{hi} cells than for CD19^{lo} B cells (statistics summarized in the legend for Figure 3). Collectively, consistent with deletion of *Notch1* in HSCs by *Mx^{Cre}*, deletion of *Notch1* in pro-T cells blocked early T cell development and was associated with the new appearance of CD19^{lo} B cells in the thymus. Unexpectedly, however, absolute numbers of both CD19^{lo} and CD19^{hi} B thymic cells increased substantially.

Cell-Intrinsic and Cell-Extrinsic *Notch1*-Dependent Mechanisms Leading to Thymic B Cells

If thymic B cells are generated by fate conversion from *Notch1*-deleted progenitors, they must be homozygous *Notch1* deleted. To obtain genotype frequencies, we established a single-cell PCR assay (see Supplemental Results for efficiency and specificity) that can distinguish homozygous floxed (*Notch1$^{fl/fl}$*), homozygous deleted (*Notch1$^{Δ/Δ}$*), and heterozygous (*Notch1$^{fl/Δ}$*) genotypes. The *Notch1* genotype was analyzed in 319 single CD19^{lo} and 272 single CD19^{hi} thymic B cells from *Notch1$^{fl/fl}$*

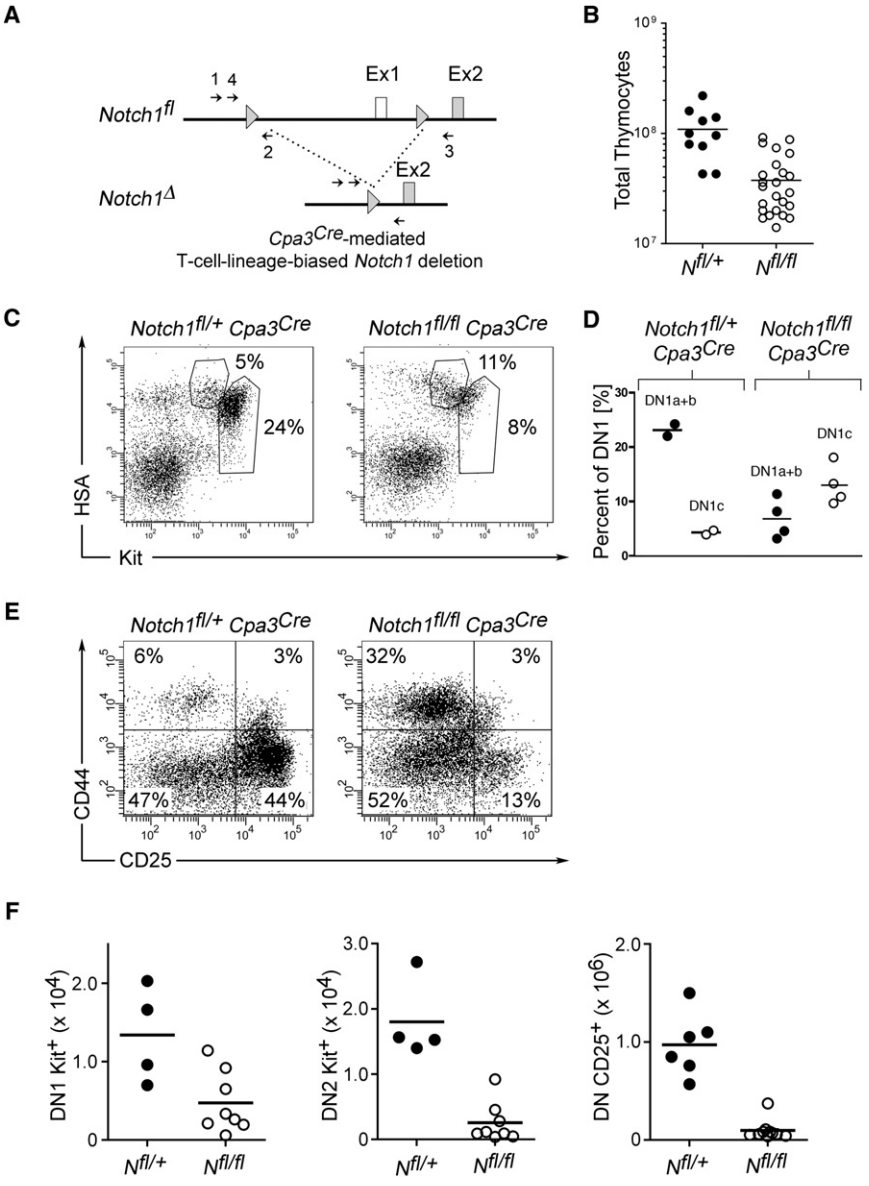

Figure 2. Impact of *Notch1* Deletion by *Cpa3*^{Cre} on T Cell Development

(A) Schematic outline of exon 1 (Ex1) and Ex2 of the *Notch1* locus, the positions of the loxP sites (triangle) in the *Notch1*^{fl} allele, and the binding sites of the oligonucleotides used for *Notch1* genotyping. The configurations of the functional nondeleted *Notch1*^{fl} and the nonfunctional deleted *Notch1*$^{\Delta}$ alleles are depicted. The ordered use of the oligonucleotides (1–4) for PCR genotyping is described in the Supplemental Data.

(B) Absolute numbers of thymocytes were determined for *Notch1*$^{fl/+}$*Cpa3*^{Cre} (abbreviated $N^{fl/+}$) mice (n = 10; 1.1 ± 0.5 × 10^8 thymocytes) and for *Notch1*$^{fl/fl}$*Cpa3*^{Cre} (abbreviated $N^{fl/fl}$) mice (n = 24; 0.38 ± 0.25 × 10^8 thymocytes) ($p < 0.05$).

(C) Lin$^-$CD44$^+$CD25$^-$ thymocytes from *Notch1*$^{fl/+}$ *Cpa3*^{Cre} and *Notch1*$^{fl/fl}$*Cpa3*^{Cre} mice were resolved into DN1a+b (HSA$^+$Kit$^+$) and DN1c (HSA^{hi}Kit^{lo}). Representative plots are shown.

(D) DN1a+b (represented by closed circles) and DN1c (represented by open circles) are shown in percent of total DN1 for *Notch1*$^{fl/+}$*Cpa3*^{Cre} and *Notch1*$^{fl/fl}$*Cpa3*^{Cre} thymi. The bar indicates the means for each cell population, and each circle represents an individual thymus.

(E) Lin$^-$ DN thymocytes from *Notch1*$^{fl/+}$*Cpa3*^{Cre} and *Notch1*$^{fl/fl}$*Cpa3*^{Cre} mice were analyzed for CD44 and CD25 expression. DN percentages in *Notch1*$^{fl/+}$*Cpa3*^{Cre} mice (n = 5) were 4.5% ± 2.1% in DN1, 3.5% ± 0.8% in DN2, 48.0% ± 5.7% in DN3, and 44.1% ± 3.7% in DN4. DN percentages in *Notch1*$^{fl/fl}$*Cpa3*^{Cre} mice (n = 11) were 21.8% ± 8.7% in DN1, 3.0% ± 1.4% in DN2, 20.8% ± 5.8% in DN3, and 54.6% ± 7.6% in DN4. Representative plots are shown.

(F) Absolute cell numbers per *Notch1*$^{fl/+}$*Cpa3*^{Cre} (abbreviated $N^{fl/+}$) thymus (represented by closed circles) or per *Notch1*$^{fl/fl}$*Cpa3*^{Cre} (abbreviated $N^{fl/fl}$) thymus (represented by open circles) were determined for total DN1 Kit$^+$ cells (1.34 ± 0.61 × 10^4 [n = 4] in *Notch1*$^{fl/+}$*Cpa3*^{Cre} versus 0.47 ± 0.38 × 10^4 [n = 8] in *Notch1*$^{fl/fl}$*Cpa3*^{Cre} [$p < 0.05$]), for Kit$^+$ DN2 cells (1.80 ± 0.61 × 10^4 [n = 4] for *Notch1*$^{fl/+}$*Cpa3*^{Cre} versus 0.25 ± 0.30 × 10^4 [n = 8] in *Notch1*$^{fl/fl}$*Cpa3*^{Cre} [$p < 0.05$]), and for CD25$^+$ (DN2+DN3) cells (9.7 ± 3.2 × 10^5 [n = 6] for *Notch1*$^{fl/+}$*Cpa3*^{Cre} versus 0.97 ± 0.99 × 10^5 [n = 10] in *Notch1*$^{fl/fl}$*Cpa3*^{Cre} [$p < 0.05$]). All mice were 6 weeks old. The bar indicates the mean for each cell population, and each circle represents an individual thymus.

Cpa3^{Cre} mice (Figure 4A). Remarkably, CD19^{lo} and CD19^{hi} thymic B cells had a fundamentally different *Notch1* genotype. Out of all CD19^{lo} B cells, 94% ± 5% were *Notch1*$^{\Delta/\Delta}$ (Figure 4B, lower panel, and Figure 4C). This frequency was similar to the deletion frequency in DN1 Kit$^+$Flt3$^+$ cells (87% *Notch1*$^{\Delta/\Delta}$ in a total of 106 cells analyzed at the single-cell level in two independent experiments). Quantitative deletion of *Notch1* specifically in CD19^{lo} B cells, but not in other B cells (see below), showed that these B cells arose from *Notch1*-deleted progenitors. This is consistent with a model of cell-intrinsic T-to-B cell fate conversion.

In marked contrast, the frequency of homozygous *Notch1* deletion in CD19^{hi} thymic B cells was only 26% ± 11% (Figure 4B, upper panel, and Figure 4C). Thus, the majority of this major B cell population was not *Notch1* deleted. Of note, this deletion frequency in CD19^{hi} thymic B cells was similar to that measured for CD19^{lo} (28% ± 10%) and CD19^{hi} (19% ± 12%) B cells isolated from the bone marrow (Figure 4C), and it was also in the range of the deletion frequency in common lymphoid progenitors (CLPs) (Lin$^-$interleukin-7-receptor$^+$Kit^{lo} Sca^{lo}) in the bone marrow. In a total of 110 CLPs analyzed at the single-cell level in two independent experiments, 13% were *Notch1*$^{\Delta/\Delta}$. These data demonstrate that the majority of cells from these three B cell populations (CD19^{hi} thymic B cells, CD19^{lo} bone marrow B cells, and CD19^{hi} bone marrow B cells) develop independently of cell-intrinsic *Notch1* deletion. Because

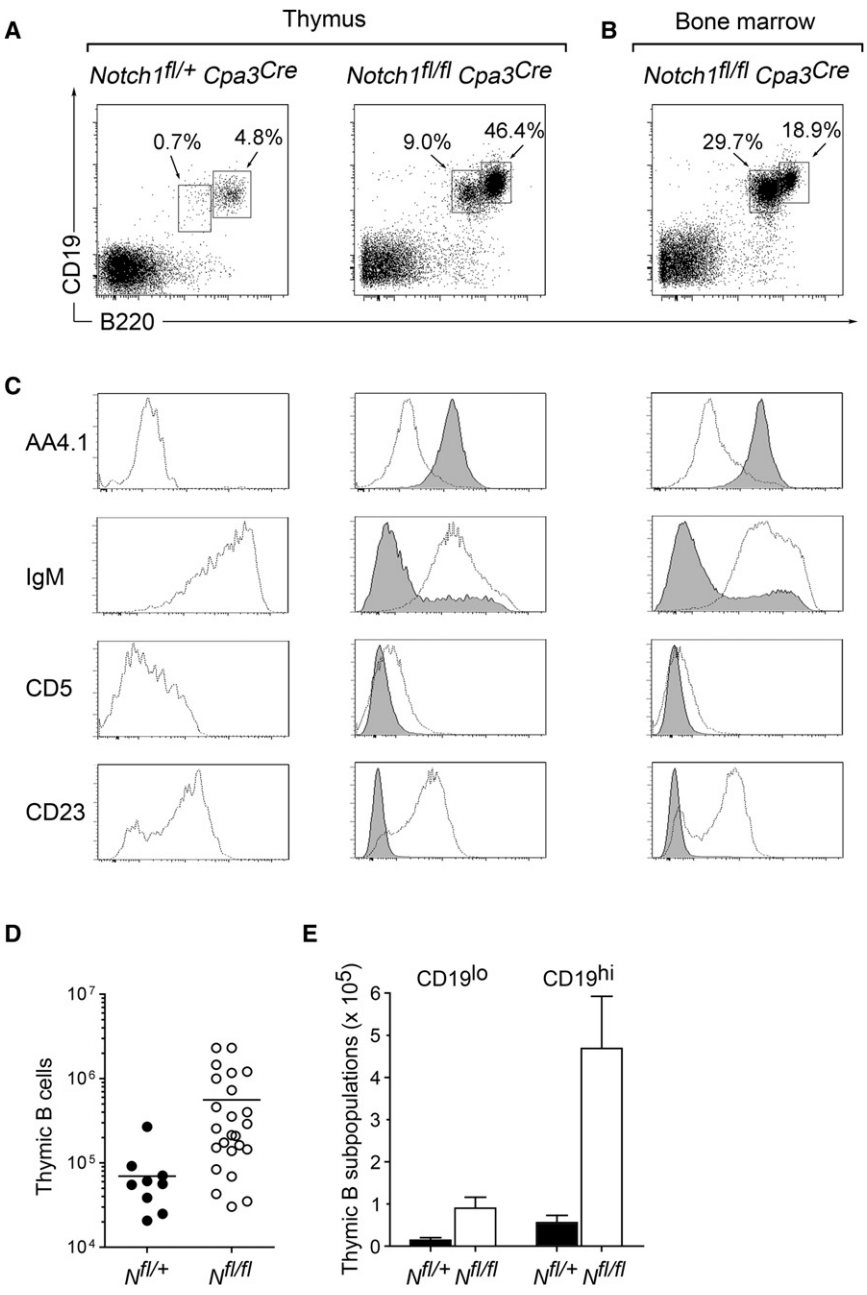

Figure 3. Deletion of *Notch1* by *Cpa3*^{Cre} Promotes Thymic B Cell Populations

(A) CD4$^-$CD8$^-$ cells from *Notch1*$^{fl/+}$*Cpa3*^{Cre} and *Notch1*$^{fl/fl}$*Cpa3*^{Cre} thymi were stained for CD19 versus B220. Percentages of CD19^{lo}B220^{lo} (termed CD19^{lo}) and of CD19^{hi}B220^{hi} (termed CD19^{hi}) B cells are shown.

(B) For comparison, CD4$^-$CD8$^-$ cells from *Notch1*$^{fl/fl}$*Cpa3*^{Cre} bone marrow were stained for CD19 versus B220.

(C) B cells from *Notch1*$^{fl/+}$*Cpa3*^{Cre} thymi (left column), *Notch1*$^{fl/fl}$*Cpa3*^{Cre} thymi (middle column), or *Notch1*$^{fl/fl}$*Cpa3*^{Cre} bone marrow (right column) were analyzed for expression of the indicated cell-surface markers. Open histograms correspond to CD19^{hi} cells from *Notch1*$^{fl/+}$*Cpa3*^{Cre} or *Notch1*$^{fl/fl}$*Cpa3*^{Cre} mice, and filled histograms correspond to CD19^{lo} cells from *Notch1*$^{fl/fl}$ *Cpa3*^{Cre} mice. CD19^{lo} cells from *Notch1*$^{fl/+}$*Cpa3*^{Cre} do not present a defined population and are therefore not shown in the histograms.

(D) Absolute numbers of thymic B cells (CD19^{lo} plus CD19^{hi}) were 6.9 ± 7.4 × 10^4 for *Notch1*$^{fl/+}$ *Cpa3*^{Cre} (n = 10) and 56 ± 68 × 10^4 *Notch1*$^{fl/fl}$ *Cpa3*^{Cre} (n = 24) mice ($p < 0.05$).

(E) Absolute numbers of CD19^{lo} B cells per thymus were 1.4 ± 2.0 × 10^4 *Notch1*$^{fl/+}$*Cpa3*^{Cre} (black bars) versus 9.0 ± 12.8 × 10^4 *Notch1*$^{fl/fl}$*Cpa3*^{Cre} (white bars) ($p < 0.05$), and absolute numbers of CD19^{hi} B cells per thymus were 5.6 ± 5.5 × 10^4 *Notch1*$^{fl/+}$*Cpa3*^{Cre} (black bars) versus 46.9 ± 60.6 × 10^4 *Notch1*$^{fl/fl}$*Cpa3*^{Cre} (white bars) ($p < 0.05$). Error bars show standard error of the mean (SEM). Mice were 6 to 10 weeks old with genotypes age matched (A–C). In (D) and (F), *Notch1*$^{fl/+}$*Cpa3*^{Cre} were analyzed at 5, 8, and 9 weeks of age, and *Notch1*$^{fl/fl}$*Cpa3*^{Cre} were analyzed at 5, 7, 8, 9, and 10 weeks of age. Data in (A), (B), (D), and (E) are representative of at least 10 mice of each genotype, and data in (C) were collected in four individual experiments.

we noted the strongest increase in absolute numbers in the CD19^{hi} thymic B cell compartment in *Notch1*$^{fl/fl}$*Cpa3*^{Cre} mice (Figure 3E), most thymic B cells arising in response to *Notch1* deletion in the T cell pathway were not products of T-to-B cell fate conversion. We refer to this as the cell-extrinsic pathway of thymic B cells. Collectively, single-cell genotyping identified *Notch1*-dependent cell-intrinsic and *Notch1*-dependent cell-extrinsic mechanisms leading to the generation of thymic B cells.

Thymic B Cells Can Arise from TCR-Rearrangement-Bearing Progenitors

To search for additional evidence that thymic B cells can originate from pro-T cells in vivo, we analyzed B cells from thymus (Figures S3A, S3B, and S4A) and bone marrow (Figures S3C, S3D, and S4B) of *Notch1*$^{fl/fl}$*Cpa3*^{Cre} mice for T cell receptor (TCR) β chain rearrangements. Essentially no TCR rearrangements were detectable in B cells from the bone marrow (Figures S3C, S3D, and S4B). In contrast, TCR Dβ1Jβ1 rearrangements, but not Dβ2Jβ2 rearrangements, were present in DNA from CD19^{lo} thymic B cells in *Notch1*$^{fl/fl}$*Cpa3*^{Cre} mice (Figures S3A and S4A). A defined and isolatable population of CD19^{lo} B cells was only present in *Notch1*$^{fl/fl}$*Cpa3*^{Cre} mice, but not in *Notch1*$^{fl/+}$*Cpa3*^{Cre} (Figure 3A) or wild-type (data not shown) mice, precluding TCR-rearrangement analyses of a corresponding population in a Notch-competent thymus. TCR rearrangements in CD19^{lo} B cells from *Notch1*$^{fl/fl}$*Cpa3*^{Cre} mice, together with the high frequency of *Notch1*$^{\Delta/\Delta}$ in these cells (Figure 4C), showed that some CD19^{lo} cells can develop from *Notch1*-deleted pro-T cells bearing Dβ1Jβ1 rearrangements. Lack of Dβ2Jβ2 rearrangements indicates that this diversion can only happen prior to the DN2 stage (see Supplemental Results).

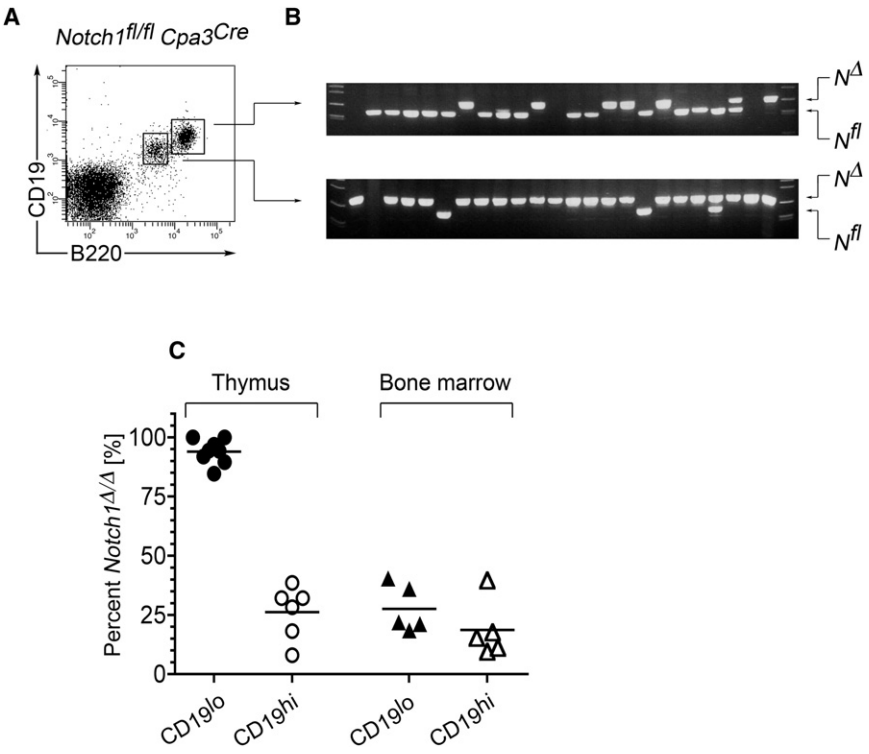

Figure 4. Single-Cell Genotyping of CD19^{lo} and CD19^{hi} Thymic B Cells

(A) CD4$^-$CD8$^-$ cells from *Notch1$^{fl/fl}$Cpa3^{Cre}* mice were gated into CD19^{hi} and CD19^{lo} thymic B cells according to the regions shown and were deposited by single-cell sorting into PCR plates.

(B) The *Notch1* genotype of single CD19^{hi} B cells (upper panel) and CD19^{lo} B cells (lower panel) was examined by nested PCR with the oligonucleotides shown in Figure 2A. Lower band, upper band, and lower plus upper band correspond to *Notch1$^{fl/fl}$*, *Notch1$^{\Delta/\Delta}$*, and *Notch1$^{fl/\Delta}$* genotypes, respectively.

(C) In *Notch1$^{fl/fl}$Cpa3^{Cre}* mice, frequencies of *Notch1$^{\Delta/\Delta}$* genotypes (in percent of all cells analyzed) are summarized for CD19^{lo} versus CD19^{hi} B cells in the thymus and for CD19^{lo} versus CD19^{hi} B cells in the bone marrow. Each symbol corresponds to the single-cell PCR analysis of one mouse, and the bar indicates the mean of the frequencies for each group of mice. Total numbers of B cells analyzed in all experiments were 319 CD19^{lo} and 272 CD19^{hi} for the thymus and 291 CD19^{lo} and 293 CD19^{hi} for the bone marrow. Mice were 7–10 weeks old.

Dβ1Jβ1 rearrangements were found only very rarely in CD19^{hi} thymic B cells from *Notch1$^{fl/fl}$Cpa3^{Cre}* mice (Figures S3A and S4A) and from wild-type mice (Figure S5). Rare TCR rearrangements, together with the low frequencies of *Notch1$^{\Delta/\Delta}$* in CD19^{hi} cells (Figure 4C), support the overall T cell-independent origin of CD19^{hi} B cells. Although we cannot exclude that some B cells can progress from CD19^{lo} to CD19^{hi} stages in *Notch1$^{fl/fl}$Cpa3^{Cre}* mice, such transition appeared to be rare (Figures S3A and S4A). Hence, in the absence of Notch1 signaling, thymic B cells can arise from TCR rearrangement-bearing progenitors, an event that apparently happens only rarely in a normal thymus and never in the bone marrow.

T Cell-Biased Deletion of *Notch1* Diverts Pro-T cells to DCs in the Thymus

On the basis of the substantial potential of the DN1 Kit$^+$ population for DCs, it has been proposed that thymic DCs and T cells share a common progenitor (Shortman and Naik, 2007). Given that thymic DCs can develop independently of pro-T cells (Di Santo et al., 2000), it remains to be determined to what extent T cells and DCs develop from a common thymic pathway in vivo and whether Notch1 signaling can influence the lineage choice between the T cell and DC fates. We took advantage of our Cre line to investigate the impact of *Notch1* deletion on potential pro-T cell-to-DC fate switching in the thymus. *Notch1$^{fl/+}$Cpa3^{Cre}* and *Notch1$^{fl/fl}$Cpa3^{Cre}* mice were bred to additionally harbor the *RFP* indicator locus. In control *Notch1$^{fl/+}$Cpa3^{Cre}RFP* mice, Cre can turn on *RFP*, but it cannot inactivate *Notch1*. In these mice, RFP-labeling frequencies of thymic DC populations should be informative about the originating progenitors when compared to labeling frequencies of DN subsets (Figure 1D). In *Notch1$^{fl/fl}$Cpa3^{Cre}RFP* mice, Cre expression can delete *Notch1* while turning on *RFP*. If deletion of *Notch1* drives pro-T cell-to-DC fate conversion in the thymus, percentages of RFP$^+$ DCs should increase in *Notch1$^{fl/fl}$Cpa3^{Cre}RFP* mice compared to those in *Notch1$^{fl/+}$Cpa3^{Cre}RFP* mice.

Thymic and splenic (Figure 5A) and bone marrow (Figure S1B) DC subpopulations were separated into "lymphoid" DCs (lyDCs), "myeloid" DCs (mDCs), and plasmacytoid DCs (pDCs) (see Supplemental Data for phenotypes) and analyzed for RFP expression (Figures 5B and 5C). In the *Notch1$^{fl/+}$Cpa3^{Cre}RFP* control thymus, 32%, 34%, and 20% of lyDCs, mDCs, and pDCs, respectively, were RFP$^+$ (Figure 5B), and similar frequencies were found in the spleen (Figure 5B) and bone marrow (Figure S1B). In the latter site, lyDCs were undetectable. For the thymus, this fate-mapping result is compatible with an origin of most thymic DCs from DN1 Kit$^+$ Flt3$^+$ cells, but not from cells of later stages.

Interestingly, frequencies of RFP$^+$ DCs increased in the thymus (Figures 5B and 5C), but not the spleen (Figures 5B and 5C) or bone marrow (data not shown) in *Notch1$^{fl/fl}$Cpa3^{Cre}RFP* mice as compared to those in *Notch1$^{fl/+}$Cpa3^{Cre}RFP*. RFP-labeled DCs went up from 32% to 61% for lyDCs, from 34% to 56% for mDCs, and from 20% to 32% for pDCs (Figure 5B). A similar increment was consistently observed for each thymic DC population in all experiments (n = 7) (Figure 5C). These changes in RFP-labeling frequencies correlated with differences in *Notch1* deletion frequencies. In thymic DCs of *Notch1$^{fl/fl}$Cpa3^{Cre}RFP* mice, frequencies of *Notch1$^{\Delta/\Delta}$* were 85% (74 cells analyzed) for lyDCs, 69% (80 cells) for mDCs, and 75% (77 cells) for pDCs. In splenic DCs, frequencies of *Notch1$^{\Delta/\Delta}$* were 54% (71 cells) for lyDCs, 32% (66 cells) for mDCs, and 20% (75 cells) for pDCs. Hence, both *Notch1* deletion and RFP expression were consistent with

a Notch1-dependent T cell-to-DC fate conversion in the thymus. In further support of a pro-T origin of some thymic DCs, TCR Dβ1Jβ1 rearrangements were detectable in DNA from lyDCs and pDCs, but not from mDCs, from the thymus of *Notch1*$^{fl/fl}$ *Cpa3*^{Cre}*RFP* mice (Figure S6). Such TCR rearrangements were absent from DC populations in the spleen of *Notch1*$^{fl/fl}$ *Cpa3*^{Cre}*RFP* mice (Figure S6) and, in agreement with earlier reports (Shortman and Naik, 2007), also from DCs in the wild-type thymus (Figure S7).

On the basis of this combination of *Notch1* deletion with fate mapping, we propose that most thymic DCs normally either originate independently of the T cell pathway or branch off no later than at the DN1 Kit$^+$ Flt3$^+$ pro-T stage. In contrast, under conditions of blocked Notch1 signaling in pro-T cells, a substantial proportion of thymic DCs can arise by pro-T cell-to-DC fate conversion. Because absolute numbers of thymic DC subsets were similar when we compared *Notch1*$^{fl/+}$*Cpa3*^{Cre}*RFP* with *Notch1*$^{fl/fl}$*Cpa3*^{Cre}*RFP* mice (data not shown), the size of thymic DC compartments appears to be regulated by mechanisms other than DC production.

Notch Ligand Delta-like 4-Deficient Thymus Epithelium Fails to Support T Cell Development

Notch1 is crucial for T cell development in vivo, but it is unknown which Notch ligand(s), expressed by thymus epithelial cells (TECs), are important for Notch1 signaling in the thymus. Several Notch and Notch ligand family members are expressed in T cell progenitors and in TECs, respectively. However, not every possible pair of Notch-Notch ligand appears to be functionally equivalent. In vitro, Dll1 can induce T cell development via Notch1 or Notch2, whereas Dll4 promotes T cell commitment only via Notch1. Hence, although Notch1 can receive T lineage-promoting signals via either Dll1 or Dll4 in vitro (Besseyrias et al., 2007), the thymic Notch ligand relevant in vivo remains unknown. We addressed this question by using nude (*Foxn1*$^{nu/nu}$) blastocyst complementation that can target homozygous null mutations to medullary and cortical TECs in vivo (Muller et al., 2005). This genetic assay is based on the fact that *Foxn1*$^{nu/nu}$ TECs have a cell-intrinsic defect that cannot be rescued by the presence of *Foxn1*$^{+/+}$ TECs (Rodewald, 2008). In a first set of experiments, we generated *Dll1*$^{LacZ/LacZ}$ embryonic stem (ES) cells → *Foxn1*$^{nu/nu}$ blastocyst chimeras. *Dll1*^{LacZ} encodes a nonfunctional allele (Hrabe de Angelis et al., 1997) that can visualize *Dll1*-expressing cells and that abrogates *Dll1* expression in the homozygous state (*Dll1*$^{LacZ/LacZ}$, termed *Dll1*$^{-/-}$). In *Dll1*$^{-/-}$ → *Foxn1*$^{nu/nu}$ chimeras, *Dll1* expression was overall restricted to thymus blood vessels (not shown). Thymus structure and T cell development were completely unaffected by the absence of *Dll1* in TECs. Moreover, grafting of the third pouch region, the tissue that hosts the thymus anlage, from day 10.5 *Dll1*$^{-/-}$ mice (Hrabe de Angelis et al., 1997) into nude mice yielded functional thymus (data not shown). We, therefore, exclude a nonredundant role of *Dll1* in thymus organogenesis or T cell development. In a second set of experiments, we used a *Dll4*^{LacZ} knockin reporter allele (Gale et al., 2004) to identify expression and function of *Dll4* in the thymus, again using nude complementation (Figure 6A). The *Dll4*^{LacZ} allele is nonfunctional (Gale et al., 2004). In contrast to when we generated chimeric mice by using *Dll1*$^{-/-}$ ES cells, we could not derive surviving pups after injection of *Dll4*$^{LacZ/LacZ}$ (termed *Dll4*$^{-/-}$) ES cells → *Foxn1*$^{nu/nu}$ blastocyst (see Discussion). We next focused our search for informative chimeras on the period between fetal day 18.5 and birth, and we succeeded in identifying two mice (one from day 18.5 and one newborn) in which thymus development beyond the "nude block" was apparent. Two thymi from *Dll4*$^{-/-}$ ES cells → *Foxn1*$^{nu/nu}$ blastocyst chimeras (termed *Dll4*$^{-/-}$ thymi) were analyzed in detail by immunofluorescence, and both yielded similar results (shown in Figure 6 for the newborn thymus). Unlike the cystic, noncomplemented *Foxn1*$^{nu/nu}$ thymus (Figure 6E), the *Dll4*$^{-/-}$ thymus presented as a three-dimensional structure made of cytokeratin$^+$ major histocompatibility complex (MHC) class II$^+$ TECs (Figure 6D). The entire thymus, but not its surrounding cytokeratin$^-$ nonthymic tissue, was strongly *LacZ*$^+$ (Figure 6B). In contrast to that in the age-matched control thymus (Figure 6C), T cell development was undetectable in the neonatal *Dll4*$^{-/-}$ thymus (Figure 6D). CD4$^+$CD8$^+$ thymocytes were lacking, but B220$^+$ B cells were likewise not present in large numbers in the neonatal *Dll4*$^{-/-}$ thymus (Figure 6D). These data suggest that expression of the Notch1 ligand Dll4 in TECs is essential for T cell development in vivo.

DISCUSSION

For shedding light on the role of Notch1 signaling in developmental fate decisions of pro-T cells in the thymus, it was necessary to couple *Notch1* deletion to the T cell pathway in vivo. We generated a new Cre knockin mutant that fortuitously showed a T cell-biased expression pattern reflecting the endogenous *Cpa3* expression in pro-T cells. *Cpa3* transcription can be regulated by GATA factors (Zon et al., 1991). A possible cascade of events could be that Notch1 signaling in pro-T cells induces GATA3 expression (Rothenberg, 2007), which, in turn, leads to *Cpa3*^{Cre} expression. Next, Cre deletes *Notch1*, setting the stage to reveal non-T cell fates of pro-T cells in their natural environment in vivo.

We used this system to combine fate mapping with conditional *Notch1* deletion, which revealed Notch1-dependent cell-intrinsic T cell-to-DC conversion in the thymus. Pro-T cells have DC potential in vitro and in adoptive-transfer experiments in vivo (Shortman and Naik, 2007), and other myeloid lineages can also be generated from thymic precursors at high frequencies in vitro (Balciunaite et al., 2005; Bell and Bhandoola, 2008; Wada et al., 2008). Moreover, latent myeloid potential in committed T cell progenitors has been elicited by ectopic cytokine signals (King et al., 2002) and by deregulation of transcription factors (Laiosa et al., 2006; Rothenberg, 2007), and it can be influenced by Notch signaling in human T cell progenitors in vitro (Dontje et al., 2006). However, it remains to be clarified to what extend, if at all, substantial numbers of thymic myeloid cells, including DCs, originate from pro-T cells in vivo. Interestingly, it has been proposed that Notch-Delta signaling puts a natural restraint on the latent myeloid potential of pro-T cells in the thymus (Laiosa et al., 2006; Rothenberg, 2007). Our experiments fully supported this idea. Under conditions permissive for Notch1 signaling, frequencies of RFP$^+$ DCs were, for all DC subsets, lower than frequencies of RFP$^+$ DN1 Kit$^+$ cells and much lower than frequencies of RFP$^+$ DN2 cells. Accordingly, the majority of thymic DCs cannot branch off later than at the

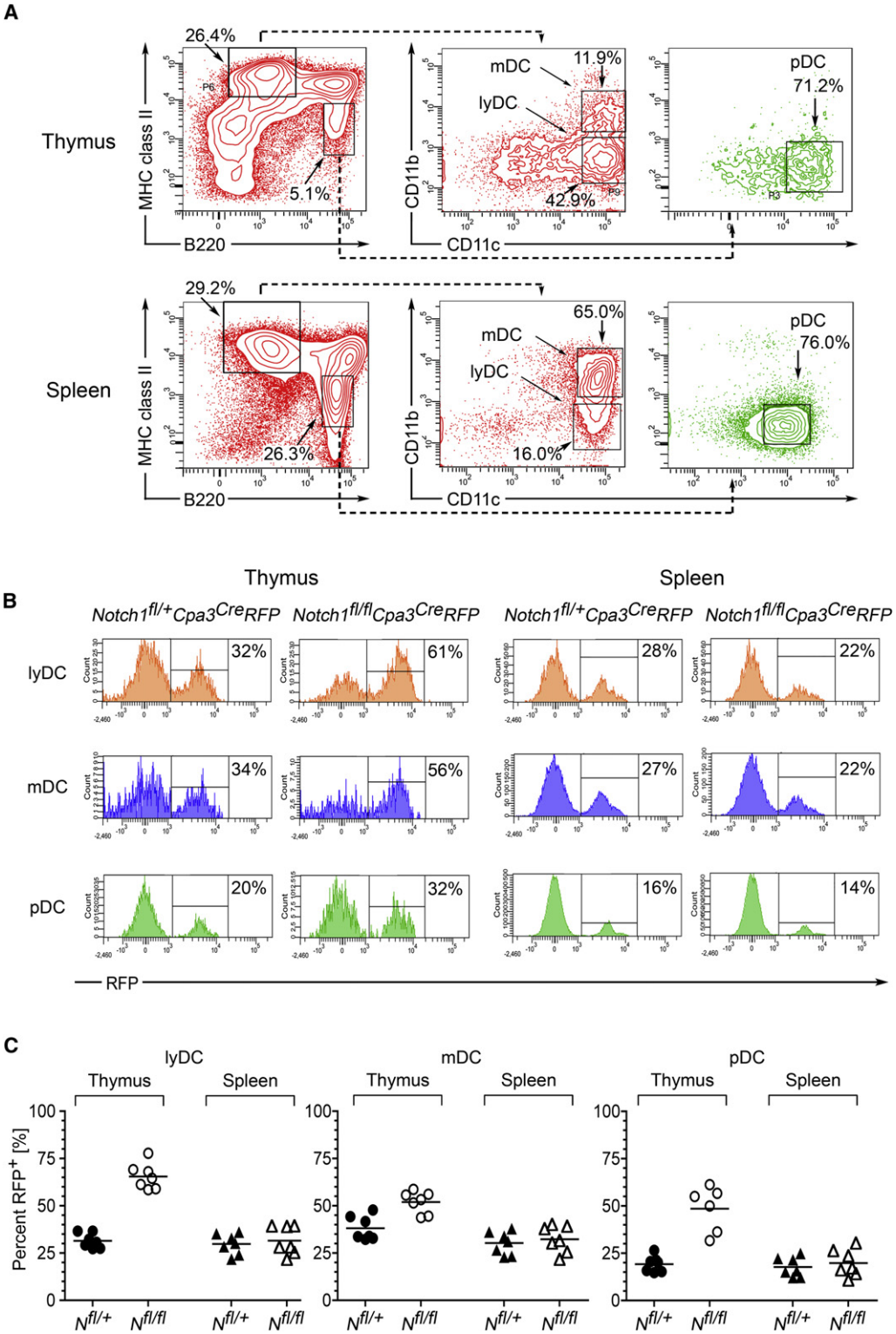

Figure 5. Combining *Notch1* Deletion with Fate Mapping Reveals Pro-T cell-to-DC Diversion in the Thymus

(A) Phenotype of analyzed thymic and splenic dendritic cell populations. DC subpopulations were gated into MHC class II^{hi}B220^{-}CD11c^{+}CD11b^{-} (lymphoid DCs, lyDC) or MHC class II^{hi}B220^{-}CD11c^{+}CD11b^{+} (myeloid DCs, mDC), or MHC class II^{lo}B220^{+}CD11c^{+}CD11b^{-} (plasmacytoid DCs, pDC). Data shown are from a *Notch1$^{fl/+}$Cpa3^{Cre}RFP* mouse, but the same DC phenotypes and distributions were seen in *Notch1$^{fl/fl}$ Cpa3^{Cre}RFP* mice. Plots are a representative example of the mice analyzed in (C).

(B) DC populations from thymus and spleen of *Notch1$^{fl/+}$Cpa3^{Cre}RFP* and *Notch1$^{fl/fl}$ Cpa3^{Cre}RFP* mice were gated as shown in (A) and analyzed for percentages of RFP-expressing cells. Histograms are representative examples for the mice summarized in (C).

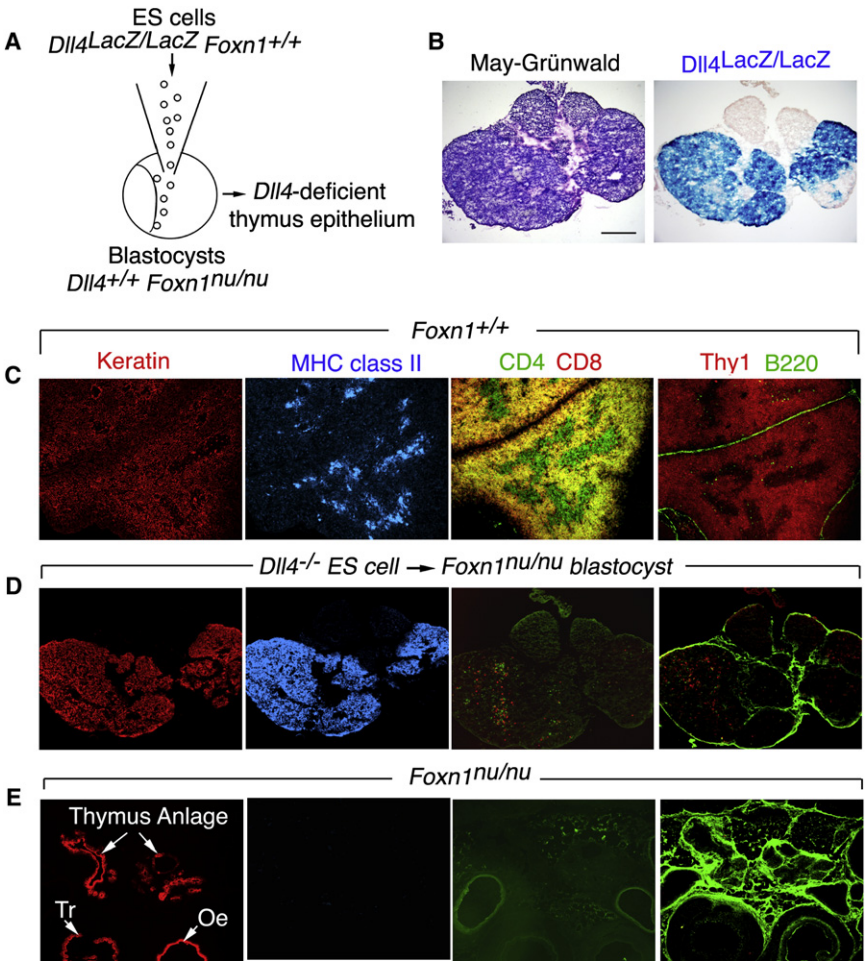

Figure 6. Analysis of the Role of *Dll4* in Thymus Epithelium by Nude Complementation

(A) Experimental outline for targeting *Dll4* deficiency into thymus epithelium in vivo. After injection of $Dll4^{-/-}$ ES cells into $Foxn1^{nu/nu}$ blastocysts, thymus epithelium in chimeric mice is exclusively of ES cell origin, not of blastocyst origin.

(B) May-Grünwald-Giemsa staining of the thymus in a newborn $Dll4^{-/-}$ into $Foxn1^{nu/nu}$ chimera (termed $Dll4^{-/-}$ thymus) and LacZ staining of the serial sections of the same thymus. Note the blue thymus and white surrounding nonthymic tissue, probably fat.

(C–E) Immunofluorescence analysis of structure and function of wild-type thymus (C), $Dll4^{-/-}$ thymus (D), and $Foxn1^{nu/nu}$ thymus (transversal section with bilateral thymus anlage, trachea, and esophagus) (E). All thymi are from newborn mice. Thymus sections (5 μm) were stained for pan-cytokeratin versus MHC class II and for CD4 versus CD8 or for Thy1 versus B220. The scale bar in (B) applies to all panels and corresponds to 200 μm. Data shown are from one out of two independent experiments, both showing lack of T cell development in the absence of Dll4 in TECs.

DN1 Kit^+Flt3^+ stage, or they normally develop independently of pro-T cells in vivo. The latter model would be in keeping with pro-T cell-independent thymic DC development (Di Santo et al., 2000). However, upon *Notch1* deletion in pro-T cells, RFP-labeling frequencies approximately doubled. Moreover, in $Notch1^{fl/fl}Cpa3^{Cre}RFP$ mice, frequencies of $Notch1^{\Delta/\Delta}$ were higher for thymic DCs than for splenic DCs, and TCR rearrangements were found in thymic DC subpopulations from $Notch1^{fl/fl}Cpa3^{Cre}RFP$ mice, but not from wild-type mice. Together, these results point at Notch1-dependent T cell-to-DC fate conversion within the thymus. Notably, all analyzed DC subtypes, earlier classified as lymphoid, myeloid, and plasmacytoid DCs, were included in this transdifferentiation process. Of these, only lyDCs and pDCs showed signs of TCR rearrangements. This is consistent with the proposal that these two lineages are close to a lymphoid origin (Shortman and Naik, 2007). According to our fate mapping, mDCs should now be included in the non-T cell potential of pro-T cells. The efficiency of pro-T cell-to-DC conversion is unknown, and it may be an infrequent event in a wild-type thymus. However, a large fraction of thymic DCs can originate from pro-T cells in vivo upon withdrawal of Notch1 signals.

Conclusions on the origins of thymic B cells under conditions of Notch1 deficiency in the hematopoietic system must consider the specificity of Notch1 targeting. Genetic inhibition of Notch1 signaling in hematopoietic cells in vivo has previously been achieved by, among other approaches, conditional ablation of *Notch1* (Radtke et al., 1999; Wilson et al., 2001; Wolfer et al., 2001), dysglycosylation of Notch1 via transgenic overexpression of lunatic fringe (*Lfng*) (Koch et al., 2001), deletion of the transcription factor recombination signal-binding protein-J (RBP-J) (Han et al., 2002), overexpression of the Notch modulator *Deltex1* (Izon et al., 2002), or interference with the transcriptional activity of *Notch1* using dominant-negative mastermind-like protein 1 (Maillard et al., 2004). In cases of global deletion in bone marrow cells (e.g., Izon et al., 2002; Maillard et al., 2004; Radtke et al., 1999; Wilson et al., 2001), loss of *Notch1* may have affected the developmental potential of HSCs, CLPs,

(C) Summary of frequencies of RFP^+ lyDCs, mDCs, and pDCs in thymi of $Notch1^{fl/+}Cpa3^{Cre}RFP$ mice (abbreviated $N^{fl/+}$; represented by closed circles) and $Notch1^{fl/fl}Cpa3^{Cre}RFP$ mice (abbreviated $N^{fl/fl}$; represented by open circles) and in the spleens of $Notch1^{fl/+}Cpa3^{Cre}RFP$ mice (abbreviated $N^{fl/+}$; represented by closed triangles) and $Notch1^{fl/fl}Cpa3^{Cre}RFP$ mice (abbreviated $N^{fl/fl}$; represented by open triangles). In the thymi, frequencies of RFP^+ cells for lyDCs, were 31.5% ± 3.9% (n = 7) in $N^{fl/+}$ mice and 65.5% ± 6.8% (n = 7) in $N^{fl/fl}$ mice ($p < 0.05$); for mDCs, 38.1% ± 6.4% (n = 7) in $N^{fl/+}$ mice and 51.9% ± 5.8% (n = 7) in $N^{fl/fl}$ mice ($p < 0.05$); and for pDCs, 19.2% ± 4.2% (n = 7) in $N^{fl/+}$ mice and 48.5% ± 11.9% (n = 6) in $N^{fl/fl}$ mice ($p < 0.05$). For the spleens, frequencies of RFP^+ cells were also determined for lyDCs (29.8% ± 5.4% in $N^{fl/+}$ [n = 7] versus 31.6% ± 7.5% in $N^{fl/fl}$ [n = 7] [p = 0.40; not significant]), for mDCs (30.3% ± 6.1% in $N^{fl/+}$ [n = 7] versus 32.3% ± 7.1% in $N^{fl/fl}$ [n = 7] [p = 0.27; not significant]), and for pDCs (17.7% ± 5.2% in $N^{fl/+}$ [n = 7] versus 19.8% ± 7.1% in $N^{fl/fl}$ [n = 7] [p = 0.27; not significant]).

committed B cells, or committed T cell progenitors. Deletion of *Notch1* inside the thymus using Lck^{Cre} (deletion completed by DN3) caused specific defects in T cell development but was possibly too late for a T-to-B cell switch (Wolfer et al., 2002).

Several conclusions emerge from these earlier studies: The first is that, in all cases of an early block in T cell development, thymic B cells appeared in increased numbers. Second, deletion of *Notch1*, or interference with Notch1 function, was not restricted to the T cell pathway, and the resulting phenotype may have been due to altered development of some or several of these populations. Third, by definition, all progeny of *Notch1*-deleted HSCs are also lacking Notch1; hence, all B cells are *Notch1* deleted, regardless of whether they developed in the bone marrow or in the thymus and whether this deletion was the underlying mechanism for their appearance in the thymus. Fourth, frequencies of B cell potential in DN1 Kit^+ cells, read out in the absence of Notch signals, are very low, ranging from 1/30 (Heinzel et al., 2007) to 1/500 (Sambandam et al., 2005) or even less (Balciunaite et al., 2005). In summary, it remained ambiguous whether B cells arising under conditions of impaired Notch1 signaling were, in fact, fate-converted descendents of committed T cell progenitors. This caveat also applies to in vitro experiments in which Notch1 signaling is compromised in progenitor populations from bone marrow or fetal liver.

This issue has now been addressed with the T cell-biased Cre deleter. Genotyping of large numbers of single thymic B cells in $Notch1^{fl/fl}Cpa3^{Cre}$ mice has now directly demonstrated that a major fraction of thymic B cells have a *Notch1* genotype inconsistent with a model of Notch-dependent T-to-B cell conversion. In keeping with low frequencies of *Notch1* deletion in CLPs and in immature and mature bone marrow B cells, the $CD19^{hi}$ thymic B cells were not quantitatively *Notch1* deleted. Because these cells do not share a precursor-product relationship with *Notch1*-deleted T cell progenitors, the effect of Notch1 on these cells is non-cell autonomous, which we refer to as cell-extrinsic. It is likely that these B cells develop in the bone marrow before migrating into the thymus. Nevertheless, we noted the strongest increment in absolute numbers in these $CD19^{hi}$ B cells in the $Notch1^{fl/fl}Cpa3^{Cre}$ thymus. One could argue that the major effect of *Notch1* deletion in pro-T cells in vivo is on the cell-extrinsic pathway rather than on fate conversion. This notion may be relevant for studies into the molecular basis of the role of Notch1 in the T-B cell fate decision (Ikawa et al., 2006; Nie et al., 2008). Evidence for a non-cell-autonomous effect of Notch deficiency on thymic B cells had also been obtained in mice overexpressing *Lfng* in thymocytes, which blocked T cell development and promoted thymic B cells (Koch et al., 2001). In chimeric experiments, thymic B cells arose not only from *Lfng*-transgenic progenitors, but instead predominantly from nontransgenic progenitors, suggesting a non-cell-autonomous mechanism (Koch et al., 2001). Withdrawal of Notch ligands in the thymus via *Lfng*-transgenic thymocytes has been proposed as a mechanism to fit these data into the fate-conversion model (Visan et al., 2006), but large numbers of non-*Lfng*-transgenic B cells more likely correspond to the non-*Notch1*-deleted B cells that arise in the cell-extrinsic pathway.

The non-cell-autonomous pathway to thymic B cells could take advantage of available free niches in the thymus. This space has been deserted because T cell development requires continuous Notch signaling (Garbe et al., 2006; Sambandam et al., 2005; Schmitt et al., 2004). Thymic B cell expansion has been noted in some, but not all, mutants affected by very early blockade of T cell development (Wilson et al., 2001). Therefore, deserted stromal niches may not fully explain the excessive B cells in the Notch-deficient thymus. An alternative explanation could be that the Notch-Delta signaling axis is a sensor for contact between thymocytes and thymus epithelium. Dll4 is strongly expressed in TECs, and Dll4-expressing TECs may receive signals from Notch1-expressing thymocytes, directly via Dll4 or indirectly via other receptors, and this could maintain "stromal conditions" fostering T cell development. In the absence of Notch-Delta wiring, the thymus microenvironment may become more permissive for B cells.

In contrast to this newly recognized cell-extrinsic pathway, *Notch1* was quantitatively deleted in the vast majority of $CD19^{lo}$ B cells in $Notch1^{fl/fl}Cpa3^{Cre}$ thymi. Consistent with this notion, RFP-labeling frequencies were also higher in $CD19^{lo}$ B cells compared to those in $CD19^{hi}$ B cells in $Notch1^{fl/fl}Cpa3^{Cre}$ *RFP* thymi (data not shown). However, RFP-labeling frequencies did not reach the *Notch1*-deletion frequencies, indicating that $Cpa3^{Cre}$ acted more efficiently on the $Notch1^{fl}$ allele than on the *ROSA26-RFP* reporter allele. We thus consider the *Notch1* genotype as the most direct molecular evidence for fate conversion of *Notch1*-deleted pro-T cells to thymic B cells and, hence, the cell-intrinsic pathway. TCR rearrangements were a clear molecular marker of the "T cell lineage past" of fate-converted B cells. High frequencies (>90%) of Cre activity were only found in T cells, not in any of the B cell populations in bone marrow, spleen, peritoneal cavity, or blood of $Cpa3^{Cre}$ mice, which can only be explained by preferential labeling of the T cell lineage after the T-B cell bifurcation. Interestingly, the *Notch1*-deletion frequency was ~90% already in the earliest thymic progenitors, raising the possibility that the deletion occurred prior to thymus homing.

It is conceivable that, in the normal thymus, not all pro-T cells receive adequate Notch1 signaling, and, occasionally, limiting Notch1 signaling may result in T-to-B cell conversion, as forced here by deletion of *Notch1* in pro-T cells. It is an open question as to whether this is accidental or useful. $CD19^{lo}$ thymic B cells may be viewed as products of transdifferentiation (Xie and Orkin, 2007) from T cell to B cell, and they may represent a reciprocal case of the remarkable B-to-T cell plasticity known from *Pax5*-deficient pre-B cells (Rolink et al., 1999) and even from mature B cells (Cobaleda et al., 2007). Despite their bona fide precursor phenotype, $CD19^{lo}$ thymic B cells from $Notch1^{fl/fl}Cpa3^{Cre}$ mice may not be very efficient, fully normal B cell precursors. In adoptive-transfer experiments, $CD19^{lo}$ thymic B cells from $Notch1^{fl/fl}Cpa3^{Cre}$ mice gave rise to mature B cells only poorly when compared to $CD19^{lo}$ pre-B cells from the bone marrow (data not shown). It remains to be determined whether T-to-B cell converted thymic B cells have fully implemented the molecular circuitry (Rothenberg, 2007) of their newly adopted B cell lineage fate.

There is little information on the physiologically relevant Notch ligands in the thymus. Ectopic expression of Dll1 or Dll4 on stromal cells can drive T cell development in vitro (Besseyrias et al., 2007; Schmitt and Zuniga-Pflucker, 2002). As determined on the basis of RT-PCR, several Notch ligands are expressed in

TECs (Jenkinson et al., 2006), but the topology of Notch ligand expression in the thymus is controversial (Heinzel et al., 2007; Schmitt et al., 2004). We have analyzed the expression of *Dll1* and *Dll4* by using knockin reporter mice. As determined on the basis of LacZ staining, *Dll1* expression is thymus blood vessel-associated rather than epithelial. In contrast, the $Dll4^{LacZ}$ knockin reporter allele (Gale et al., 2004) showed very strong and ubiquitous expression of *Dll4* in the entire thymus. This expression pattern is consistent with in situ hybridization data (Heinzel et al., 2007). *Dll1*-deficient TECs did not show any defects in support of T cell development, which is in agreement with conditional deletion of Dll1 (Hozumi et al., 2004). Regarding the function of Dll4 in vivo, we reached a limitation of the nude-complementation assay. Presumably owing to the massive requirement for Dll4 expression in vasculogenesis (Duarte et al., 2004; Gale et al., 2004), we could not derive surviving pups after injection of $Dll4^{-/-}$ ES cells into 285 $Foxn1^{nu/nu}$ blastocysts, transferred into 24 foster mothers. This is reminiscent of the very low number of viable $Dll4^{+/-}$ mice (3 out of >300 offspring) derived from chimeric founders (Gale et al., 2004), and it suggests that $Dll4^{-/-}$ ES cells may be "toxic" during development even in the presence of blastocyst-derived $Dll4^{+/+}$ cells. Despite these hurdles, we obtained two informative $Dll4^{-/-}$ thymi. Unlike the cystic nude thymus, $Dll4^{-/-}$ thymi had a three-dimensional structure composed of cytokeratin$^+$MHC class II$^+$ TECs, but $Dll4^{-/-}$ thymi could not support T cell development. In contrast to adult thymi lacking *Notch1*, B220$^+$ B cells were also rare. It remains to be determined whether this difference is related to newborn versus adult age. Although we cannot rule out the possibility that *Dll4* deficiency in other organs contributed indirectly to the observed phenotype in these chimeras, these experiments show (1) that *Dll4* is very strongly expressed in TECs throughout the thymus and (2) that thymus development beyond the nude block is permissive in the absence of *Dll4* expression in TECs, and they suggest (3) that *Dll4* is essential for T cell development in vivo.

In summary, this work has shown that Notch1 expression constrains latent potential of pro-T cells toward DC and B cell lineages in the thymus. Moreover, caution may be warranted in the interpretation of Notch-deletion experiments that lead to the appearance of unusual cell types because only complex genetic and cellular separation may reveal whether such phenomena indeed reflect Notch-dependent fate conversion or represent passenger cells that take advantage of the Notch block in another lineage.

EXPERIMENTAL PROCEDURES

Mice

Mice bearing a conditional (floxed) *Notch1* allele (Radtke et al., 1999) and C57BL/6-Gt(ROSA)26Sor^{tm1Hjf} reporter mice expressing tandem-dimer RFP in a Cre-dependent manner (Luche et al., 2007) have been described. The *Cpa3* locus was targeted in ES cells for inserting Cre into the first exon of the *Cpa3* gene (Supplemental Data), and targeted ES cells were used for generating $Cpa3^{Cre}$ mice (to be designated Cpa3^{tm3Hrr}). $Dll1^{LacZ}$ and $Dll4^{LacZ}$ null alleles have been described (Gale et al., 2004; Hrabe de Angelis et al., 1997). $Dll1^{-/-}$ ES cells were derived from blastocysts obtained from intercrosses of Dll1$^{+/-}$ mice. Nude blastocyst complementation was done by injecting Dll1$^{-/-}$ or Dll4$^{-/-}$ (Gale et al., 2004) ES cells into "Black-nude" (Taconic), or "Swiss-nude" (Charles River) blastocysts as described (Muller et al., 2005).

Flow Cytometry and Histology

Antibodies used are listed in the Supplemental Data. Cells were stained for flow cytometry as described (Rodewald et al., 1997) and sorted or analyzed on FACS Aria or CantoII instruments (BD Bioscience), respectively. For histology, whole E18.5 or newborn pups were killed, placed in OCT, and snap frozen in liquid nitrogen. Transversal sections of 5 μm were cut, acetone fixed, and stored at −70°C. Thymi were removed and snap frozen in OCT on dry ice. 5 μm cryosections were treated as above and further analyzed by immunofluorescence or for β-galactosidase histochemistry (Supplemental Data). For DC analysis, thymus and spleen were digested as described in the Supplemental Data, and the released DCs were analyzed by flow cytometry as indicated in Figure 5.

RT-PCR

RNA was prepared with RNAzol B (WAK-Chemie) followed by chloroform extraction and RNA precipitation. Complimentary DNA (cDNA) was generated with the SuperScript First Strand Synthesis System (Invitrogen). RT-PCR conditions and oligonucleotides used to amplify *Cpa3* and *Actb* are stated in the Supplemental Data.

Notch1 Genotyping of Single Cells

Cells were sorted with the single-cell sorting mode (FACS Aria) and directly deposited at one cell per well into PCR plates containing 25 μl 1× PCR buffer (buffer 1 of the Expand Long Template PCR System, Roche) with 0.5mg/ml proteinase K (Invitrogen). Cells were digested by proteinase K at 50°C for 1 hr, and the enzyme was inactivated at 95°C for 10 min. The genotype of single cells was analyzed by nested PCR. PCR conditions and oligonucleotides are given in the Supplemental Data.

Analysis of TCR Rearrangements

B cells were sorted as CD4$^-$CD8$^-$CD19^{lo}B220^{lo} or CD4$^-$CD8$^-$CD19^{hi}B220^{hi} cells from bone marrow or thymus, and DP thymocytes were sorted as CD4$^+$CD8$^+$ cells from thymus. For avoiding possible contamination from thymocytes, B cells were double sorted, and dead cells were excluded via Sytox blue (Invitrogen). No thymocytes were detectable upon reanalysis of sorted B cells. In the second sort, 200 cells were deposited into 25 μl 1× PCR buffer and digested as described above for single-cell PCR. PCR analyses for TCR Dβ1 to Jβ1 and TCR Dβ2 to Jβ2 rearrangements were done as described in the Supplemental Data or as reported earlier (Rodewald et al., 1997), respectively.

Statistical Analysis

Unless stated otherwise, average data are expressed as mean ± one standard deviation. p values were calculated with the Mann-Whitney-test, and $p < 0.05$ was considered significant.

SUPPLEMENTAL DATA

Supplemental Data include Supplemental Results, Supplemental Experimental Procedures, and three figures and can be found with this article online at http://www.immunity.com/supplemental/S1074-7613(08)00542-6.

ACKNOWLEDGMENTS

We thank A. Rolink for advice on B cell populations, A. Singer for insightful discussions, S. Schlenner for critical reading of the manuscript, C. Costa for expert technical assistance, and C. Tannert and the animal facility for animal husbandry. Supported by grants from the Deutsche Forschungsgemeinschaft (SFB 497-B5 and KFO 142-P8 to H.R.R. and SFB 497-A7 to H.J.F.). N.W.G. is an employee and shareholder of Regeneron Pharmaceuticals.

Received: July 25, 2008
Revised: September 25, 2008
Accepted: October 20, 2008
Published online: December 24, 2008

REFERENCES

Artavanis-Tsakonas, S., Rand, M.D., and Lake, R.J. (1999). Notch signaling: Cell fate control and signal integration in development. Science *284*, 770–776.

Aster, J.C., Pear, W.S., and Blacklow, S.C. (2008). Notch signaling in leukemia. Annu. Rev. Pathol. *3*, 587–613.

Balciunaite, G., Ceredig, R., and Rolink, A.G. (2005). The earliest subpopulation of mouse thymocytes contains potent T, significant macrophage, and natural killer cell but no B-lymphocyte potential. Blood *105*, 1930–1936.

Bell, J.J., and Bhandoola, A. (2008). The earliest thymic progenitors for T cells possess myeloid lineage potential. Nature *452*, 764–767.

Benz, C., Martins, V.C., Radtke, F., and Bleul, C.C. (2008). The stream of precursors that colonizes the thymus proceeds selectively through the early T lineage precursor stage of T cell development. J. Exp. Med. *205*, 1187–1199.

Besseyrias, V., Fiorini, E., Strobl, L.J., Zimber-Strobl, U., Dumortier, A., Koch, U., Arcangeli, M.L., Ezine, S., Macdonald, H.R., and Radtke, F. (2007). Hierarchy of Notch-Delta interactions promoting T cell lineage commitment and maturation. J. Exp. Med. *204*, 331–343.

Bhandoola, A., Sambandam, A., Allman, D., Meraz, A., and Schwarz, B. (2003). Early T lineage progenitors: New insights, but old questions remain. J. Immunol. *171*, 5653–5658.

Bhandoola, A., von Boehmer, H., Petrie, H.T., and Zuniga-Pflucker, J.C. (2007). Commitment and developmental potential of extrathymic and intrathymic T cell precursors: Plenty to choose from. Immunity *26*, 678–689.

Ciofani, M., and Zuniga-Pflucker, J.C. (2007). The thymus as an inductive site for T lymphopoiesis. Annu. Rev. Cell Dev. Biol. *23*, 463–493.

Cobaleda, C., Jochum, W., and Busslinger, M. (2007). Conversion of mature B cells into T cells by dedifferentiation to uncommitted progenitors. Nature *449*, 473–477.

Di Santo, J.P., Radtke, F., and Rodewald, H.R. (2000). To be or not to be a pro-T? Curr. Opin. Immunol. *12*, 159–165.

Dontje, W., Schotte, R., Cupedo, T., Nagasawa, M., Scheeren, F., Gimeno, R., Spits, H., and Blom, B. (2006). Delta-like1-induced Notch1 signaling regulates the human plasmacytoid dendritic cell versus T-cell lineage decision through control of GATA-3 and Spi-B. Blood *107*, 2446–2452.

Duarte, A., Hirashima, M., Benedito, R., Trindade, A., Diniz, P., Bekman, E., Costa, L., Henrique, D., and Rossant, J. (2004). Dosage-sensitive requirement for mouse Dll4 in artery development. Genes Dev. *18*, 2474–2478.

Dumortier, A., Wilson, A., MacDonald, H.R., and Radtke, F. (2005). Paradigms of notch signaling in mammals. Int. J. Hematol. *82*, 277–284.

Gale, N.W., Dominguez, M.G., Noguera, I., Pan, L., Hughes, V., Valenzuela, D.M., Murphy, A.J., Adams, N.C., Lin, H.C., Holash, J., et al. (2004). Haploinsufficiency of delta-like 4 ligand results in embryonic lethality due to major defects in arterial and vascular development. Proc. Natl. Acad. Sci. USA *101*, 15949–15954.

Garbe, A.I., Krueger, A., Gounari, F., Zuniga-Pflucker, J.C., and von Boehmer, H. (2006). Differential synergy of Notch and T cell receptor signaling determines alphabeta versus gammadelta lineage fate. J. Exp. Med. *203*, 1579–1590.

Han, H., Tanigaki, K., Yamamoto, N., Kuroda, K., Yoshimoto, M., Nakahata, T., Ikuta, K., and Honjo, T. (2002). Inducible gene knockout of transcription factor recombination signal binding protein-J reveals its essential role in T versus B lineage decision. Int. Immunol. *14*, 637–645.

Heinzel, K., Benz, C., Martins, V.C., Haidl, I.D., and Bleul, C.C. (2007). Bone marrow-derived hemopoietic precursors commit to the T cell lineage only after arrival in the thymic microenvironment. J. Immunol. *178*, 858–868.

Hozumi, K., Negishi, N., Suzuki, D., Abe, N., Sotomaru, Y., Tamaoki, N., Mailhos, C., Ish-Horowicz, D., Habu, S., and Owen, M.J. (2004). Delta-like 1 is necessary for the generation of marginal zone B cells but not T cells in vivo. Nat. Immunol. *5*, 638–644.

Hrabe de Angelis, M., McIntyre, J., 2nd, and Gossler, A. (1997). Maintenance of somite borders in mice requires the Delta homologue Dll1. Nature *386*, 717–721.

Ikawa, T., Kawamoto, H., Goldrath, A.W., and Murre, C. (2006). E proteins and Notch signaling cooperate to promote T cell lineage specification and commitment. J. Exp. Med. *203*, 1329–1342.

Izon, D.J., Aster, J.C., He, Y., Weng, A., Karnell, F.G., Patriub, V., Xu, L., Bakkour, S., Rodriguez, C., Allman, D., and Pear, W.S. (2002). Deltex1 redirects lymphoid progenitors to the B cell lineage by antagonizing Notch1. Immunity *16*, 231–243.

Jenkinson, E.J., Jenkinson, W.E., Rossi, S.W., and Anderson, G. (2006). The thymus and T-cell commitment: The right niche for Notch? Nat. Rev. Immunol. *6*, 551–555.

King, A.G., Kondo, M., Scherer, D.C., and Weissman, I.L. (2002). Lineage infidelity in myeloid cells with TCR gene rearrangement: A latent developmental potential of proT cells revealed by ectopic cytokine receptor signaling. Proc. Natl. Acad. Sci. USA *99*, 4508–4513.

Koch, U., Lacombe, T.A., Holland, D., Bowman, J.L., Cohen, B.L., Egan, S.E., and Guidos, C.J. (2001). Subversion of the T/B lineage decision in the thymus by lunatic fringe-mediated inhibition of Notch-1. Immunity *15*, 225–236.

Laiosa, C.V., Stadtfeld, M., Xie, H., de Andres-Aguayo, L., and Graf, T. (2006). Reprogramming of committed T cell progenitors to macrophages and dendritic cells by C/EBP alpha and PU.1 transcription factors. Immunity *25*, 731–744.

Luche, H., Weber, O., Nageswara Rao, T., Blum, C., and Fehling, H.J. (2007). Faithful activation of an extra-bright red fluorescent protein in "knock-in" Cre-reporter mice ideally suited for lineage tracing studies. Eur. J. Immunol. *37*, 43–53.

Maillard, I., Fang, T., and Pear, W.S. (2005). Regulation of lymphoid development, differentiation, and function by the Notch pathway. Annu. Rev. Immunol. *23*, 945–974.

Maillard, I., Weng, A.P., Carpenter, A.C., Rodriguez, C.G., Sai, H., Xu, L., Allman, D., Aster, J.C., and Pear, W.S. (2004). Mastermind critically regulates Notch-mediated lymphoid cell fate decisions. Blood *104*, 1696–1702.

Muller, S.M., Terszowski, G., Blum, C., Haller, C., Anquez, V., Kuschert, S., Carmeliet, P., Augustin, H.G., and Rodewald, H.R. (2005). Gene targeting of VEGF-A in thymus epithelium disrupts thymus blood vessel architecture. Proc. Natl. Acad. Sci. USA *102*, 10587–10592.

Nie, L., Perry, S.S., Zhao, Y., Huang, J., Kincade, P.W., Farrar, M.A., and Sun, X.H. (2008). Regulation of lymphocyte development by cell-type-specific interpretation of Notch signals. Mol. Cell. Biol. *28*, 2078–2090.

Osborne, B.A. (2000). Transcriptional control of T cell development. Curr. Opin. Immunol. *12*, 301–306.

Petrie, H.T., and Kincade, P.W. (2005). Many roads, one destination for T cell progenitors. J. Exp. Med. *202*, 11–13.

Porritt, H.E., Rumfelt, L.L., Tabrizifard, S., Schmitt, T.M., Zuniga-Pflucker, J.C., and Petrie, H.T. (2004). Heterogeneity among DN1 prothymocytes reveals multiple progenitors with different capacities to generate T cell and non-T cell lineages. Immunity *20*, 735–745.

Pui, J.C., Allman, D., Xu, L., DeRocco, S., Karnell, F.G., Bakkour, S., Lee, J.Y., Kadesch, T., Hardy, R.R., Aster, J.C., and Pear, W.S. (1999). Notch1 expression in early lymphopoiesis influences B versus T lineage determination. Immunity *11*, 299–308.

Radtke, F., Wilson, A., Mancini, S.J., and MacDonald, H.R. (2004). Notch regulation of lymphocyte development and function. Nat. Immunol. *5*, 247–253.

Radtke, F., Wilson, A., Stark, G., Bauer, M., van Meerwijk, J., MacDonald, H.R., and Aguet, M. (1999). Deficient T cell fate specification in mice with an induced inactivation of Notch1. Immunity *10*, 547–558.

Rajewsky, K., Gu, H., Kuhn, R., Betz, U.A., Muller, W., Roes, J., and Schwenk, F. (1996). Conditional gene targeting. J. Clin. Invest. *98*, 600–603.

Reynolds, D.S., Stevens, R.L., Gurley, D.S., Lane, W.S., Austen, K.F., and Serafin, W.E. (1989). Isolation and molecular cloning of mast cell carboxypeptidase A. A novel member of the carboxypeptidase gene family. J. Biol. Chem. *264*, 20094–20099.

Robey, E.A., and Bluestone, J.A. (2004). Notch signaling in lymphocyte development and function. Curr. Opin. Immunol. *16*, 360–366.

Rodewald, H.-R. (1995). Pathways from hematopoietic stem cells to thymocytes. Curr. Opin. Immunol. *7*, 176–187.

Rodewald, H.-R., Dessing, M., Dvorak, A.M., and Galli, S.J. (1996). Identification of a committed precursor for the mast cell lineage. Science *271*, 818–822.

Rodewald, H.R. (2008). Thymus organogenesis. Annu. Rev. Immunol. *26*, 355–388.

Rodewald, H.R., Ogawa, M., Haller, C., Waskow, C., and DiSanto, J.P. (1997). Pro-thymocyte expansion by c-kit and the common cytokine receptor gamma chain is essential for repertoire formation. Immunity *6*, 265–272.

Rolink, A.G., Nutt, S.L., Melchers, F., and Busslinger, M. (1999). Long-term in vivo reconstitution of T-cell development by Pax5-deficient B-cell progenitors. Nature *401*, 603–606.

Rothenberg, E.V. (2007). Negotiation of the T lineage fate decision by transcription-factor interplay and microenvironmental signals. Immunity *26*, 690–702.

Rothenberg, E.V., Moore, J.E., and Yui, M.A. (2008). Launching the T-cell-lineage developmental programme. Nat. Rev. Immunol. *8*, 9–21.

Sambandam, A., Maillard, I., Zediak, V.P., Xu, L., Gerstein, R.M., Aster, J.C., Pear, W.S., and Bhandoola, A. (2005). Notch signaling controls the generation and differentiation of early T lineage progenitors. Nat. Immunol. *6*, 663–670.

Schmitt, T.M., Ciofani, M., Petrie, H.T., and Zuniga-Pflucker, J.C. (2004). Maintenance of T cell specification and differentiation requires recurrent notch receptor-ligand interactions. J. Exp. Med. *200*, 469–479.

Schmitt, T.M., and Zuniga-Pflucker, J.C. (2002). Induction of T cell development from hematopoietic progenitor cells by delta-like-1 in vitro. Immunity *17*, 749–756.

Shortman, K., and Naik, S.H. (2007). Steady-state and inflammatory dendritic-cell development. Nat. Rev. Immunol. *7*, 19–30.

Taghon, T., Yui, M.A., and Rothenberg, E.V. (2007). Mast cell lineage diversion of T lineage precursors by the essential T cell transcription factor GATA-3. Nat. Immunol. *8*, 845–855.

Tan, J.B., Visan, I., Yuan, J.S., and Guidos, C.J. (2005). Requirement for Notch1 signals at sequential early stages of intrathymic T cell development. Nat. Immunol. *6*, 671–679.

Tanigaki, K., and Honjo, T. (2007). Regulation of lymphocyte development by Notch signaling. Nat. Immunol. *8*, 451–456.

Visan, I., Tan, J.B., Yuan, J.S., Harper, J.A., Koch, U., and Guidos, C.J. (2006). Regulation of T lymphopoiesis by Notch1 and Lunatic fringe-mediated competition for intrathymic niches. Nat. Immunol. *7*, 634–643.

Wada, H., Masuda, K., Satoh, R., Kakugawa, K., Ikawa, T., Katsura, Y., and Kawamoto, H. (2008). Adult T-cell progenitors retain myeloid potential. Nature *452*, 768–772.

Wilson, A., MacDonald, H.R., and Radtke, F. (2001). Notch 1-deficient common lymphoid precursors adopt a B cell fate in the thymus. J. Exp. Med. *194*, 1003–1012.

Wolfer, A., Bakker, T., Wilson, A., Nicolas, M., Ioannidis, V., Littman, D.R., Lee, P.P., Wilson, C.B., Held, W., MacDonald, H.R., and Radtke, F. (2001). Inactivation of Notch 1 in immature thymocytes does not perturb CD4 or CD8 T cell development. Nat. Immunol. *2*, 235–241.

Wolfer, A., Wilson, A., Nemir, M., MacDonald, H.R., and Radtke, F. (2002). Inactivation of Notch1 impairs VDJbeta rearrangement and allows pre-TCR-independent survival of early alpha beta Lineage Thymocytes. Immunity *16*, 869–879.

Xie, H., and Orkin, S.H. (2007). Immunology: Changed destiny. Nature *449*, 410–411.

Zon, L.I., Gurish, M.F., Stevens, R.L., Mather, C., Reynolds, D.S., Austen, K.F., and Orkin, S.H. (1991). GATA-binding transcription factors in mast cells regulate the promoter of the mast cell carboxypeptidase A gene. J. Biol. Chem. *266*, 22948–22953.